Desalination and Water Treatment
www.deswater.com

doi: 10.1080/19443994.2014.941011

56 (2015) 929–938
October

Taylor & Francis
Taylor & Francis Group

Synthesizing attapulgite-graft-polyacrylamide flocculant and immobilizing microorganisms to treat low-ammonium water

Xian Xiao[a], Chaopeng Song[a], Pu Yue[b], Yuan Zhao[a], Xiang Liu[c], Yuting Liang[d,*]

[a]*School of Environment and Safety Engineering, Changzhou University, Changzhou 213164, Jiangsu, China, Tel. +86 15061971169; email: xiaoxianivy@163.com (X. Xiao), Tel. +86 13685217965; email: suxun8710@163.com (C. Song), Tel. +86 519 86330086; email: zhaoyuan12@tsinghua.org.cn (Y. Zhao)*
[b]*Department of Civil and Environmental Engineering, Northeastern University, Boston, MA 02115, USA, Tel. +86 519 86330086; email: rupert.score@gmail.com (P.Yue)*
[c]*School of Environment, Tsinghua University, Beijing 100084, China, Tel. +86 10 62783085; email: x.liu@tsinghua.edu.cn (X.Liu)*
[d]*State Key Laboratory of Soil and Sustainable Agriculture, Institute of Soil Science, Chinese Academy of Sciences, No. 71 East Beijing Road, Nanjing 210008, China, Tel. +86 25 86881534; email: msliangyuting@foxmail.com (Y.Liang)*

Received 17 December 2013; Accepted 28 June 2014

ABSTRACT

Low concentrations of ammonium are difficult to remove from surface water through traditional adsorption, air stripping, and biological techniques. Hence, we flocculate attapulgite-graft-polyacrylamide (ATP-g-PAM) and immobilize cells in this study to purify low-ammonia surface water. ATP-g-PAM was synthesized by grafting the polymerization reaction of ATP and acrylamide (AM). In this process, $FeSO_4$ and $NaHSO_3$ acted as initiators. The optimum reaction conditions were as follows: 15% AM monomer, 2% ATP, 10.5×10^{-4} mol/mol AM initiator concentration with a 1:5 molar ratio of $FeSO_4$ to $NaHSO_3$, and 5 h reaction time. The ATP-g-PAM structure was characterized further by Fourier transform infrared spectra, thermogravimetric analysis, scanning electron microscopy, and transmission electron microscopy. Results indicated that AM monomers were successfully grafted onto the ATP surface. Pellets of ATP-g-PAM-bound nitrifying bacteria were manufactured for surface water treatment. The ammonia-nitrogen removal rate ranged from 14.9 to 33.9% for adsorption and flocculation and from 69.4 to 82.6% under cell immobilization. Post-treatment, ammonia-nitrogen was less than 0.8 mg/L. Therefore, ATP-g-PAM can be an ideal carrier material of microbial fixations in water and wastewater treatment because the double-action of adsorption and flocculation induced by ATP-g-PAM can supplement the removal of pollutants.

Keywords: ATP-g-PAM; Flocculation; Immobilization; Ammonium removal

---

1. Introduction

In China, high nitrogen levels are a major aspect of urban water pollution and have frequently been detected in some old cities with dense population. These extremely high concentrations of nitrogen compounds are attributed to domestic waste discharge [1,2]. Nitrogen is generated by compounds in both organic and inorganic forms. Among these forms, ammonia nitrogen is a critical inorganic pollutant.

---

*Corresponding author.

However, ammonium is particularly difficult to remove from surface waters with low ammonium concentration, such as urban rivers. In practice, nitrogen removal methods usually involve physical, chemical, and biological processes. Typical physical and chemical methods include air stripping [3], chemical precipitation [4,5], and ion exchange [6]. Nonetheless, these methods are operationally costly and complex. Biological methods [7,8] utilize the benign process of microbial metabolism to eliminate nitrogen at relatively low cost while matching the removal rates of physical and chemical processes. Moreover, it does not produce secondary pollutants. Given the abovementioned traits, the biological removal of nitrogen is efficient and economic.

Microbial immobilization [9] confines functional enzymes or microorganisms in carrier materials, especially polymers [10–12]. During immobilization, cell unit concentration is increased and metabolic activity level is preserved [13,14]. The immobilized microorganisms metabolize and multiply rapidly. Hence, they can remove ammonia nitrogen efficiently [15], particularly when they are used to treat water with low amounts of contaminants. Hence, the required materials are low-cost, display low levels of bio-toxicity, widely available, and environment friendly [16–18]. Furthermore, a combination of physical and chemical techniques, such as flocculation and microbial immobilization, is an effective method to effectively remove ammonium nitrogen from water.

Flocculation is an important water treatment method in which dispersed particles form enlarged clusters through contact and adhesion. Flocculation is synonymous with agglomeration, aggregation, and coagulation/coalescence. As a flocculation agent, polyacrylamide (PAM) is a linear, water-soluble polymer used in water treatment to produce large floccules fast [19–21]. The lateral group of PAM polymer chains is composed of acrylamide (AM), which is highly polar and can form hydrogen bonds. To enhance the stability and effectiveness of the flocculant, other substrates [22–24] can be grafted to PAM. For instance, attapulgite (ATP) can serve as the core of a micro-crosslinking polymer system.

ATP clay [25] is a highly adsorbent earth material that is often applied in water pollution treatment. ATP clay contains micro pores and possesses a unique chain-and-layer crystalline structure. Moreover, it has large internal and external specific surface areas measuring approximately 300 and 23 m^2/g, respectively, given its specific crystal morphology, inherent pore and channel structures, and depositional pathways. In addition, ATP activation induces surface charge imbalance as a result of unusual atom sorting. This imbalance causes active sorption sites to form. Aside from the aforementioned characteristics, ATP is non-toxic, odor-free, non-stimulating, and chemically stable. Furthermore, it dries quickly and displays low hardness. Therefore, ATP is commonly used to address water pollution [26–28]. On the surfaces of ATP particles, silicone hydroxyls have a strong affinity for organic substrates [29]. Thus, ATP-PAM is a viable composite flocculant theoretically.

Based on the unique crystalline morphology and activation characteristics of ATP, grafting is initiated by mixing transition metal salt and sodium bisulfite at room temperature under air atmosphere. The resultant hybrid flocculant with organic/inorganic components is known as attapulgite-graft-polyacrylamide (ATP-g-PAM). This flocculant is then synthesized via an *in situ* reaction of intercalation polymerization [30–32].

In this study, we aim to immobilize the nitrogen-removing microbes through flocculation. In the process, we produce a pellet form of immobilized bacteria. Moreover, we combine flocculation and immobilization to treat polluted urban rivers. In the first stage of adsorption and flocculation, we used has acid-modified ATP to partially remove ammonium. In the second stage, we removed nitrogen biologically through the metabolism of ATP-g-PAM-bound bacteria.

2. Materials and methods

2.1. Preparation of the ATP-g-PAM flocculant

We first acid-modified ATP (Jiuchuan Nanomaterial Technologies Company Limited, Xuyi, Jiangsu, China) as follows: Blocks of ATP ore were ground into powder and then sieved (200 mesh). The powder was then washed with 4 M HCl, rinsed multiple times with distilled water, dried in a vacuum at 110℃ for 48 h, cooled in a cooling vessel, and finally stored in an airtight jar.

To determine the synthesis condition of the ATP-g-PAM flocculant, we optimized the effects of AM monomer mass (10–20%), initiator concentration (1:5 of $FeSO_4$ and $NaHSO_3$ with a final concentration ranging from 7×10^{-4} to 21×10^{-4} mol/mol AM), amount of ATP mass loading (0.5–3% of AM), and reaction time (2–6 h). The ATP powder was added to distilled water, sonicated for 30 min, mixed with AM, and then stirred vigorously. The initiator was then incorporated, and the mixture was incubated in a thermostatic water bath at 35℃ for 2–6 h. The resultant ATP-g-PAM flocculant was then twice-washed with absolute ethanol to remove residual AM and vacuum-dried at 50–60℃ to stabilize the weight. The experiment was conducted in triplicate.

2.2. Characterization of ATP-g-PAM

Viscose flocculants are generally adsorbent. Thus, we obtained viscosity readings at the end of graft reaction using a Brookfield Viscometer (Brookfield Laboratory Engineering, Inc., USA) to determine the viscosity of the ATP-g-PAM and to optimize and assess its performance.

We evaluated the grafting of ATP to PAM through characterization with Fourier transform infrared (FTIR) spectra. We ground ATP, PAM, and ATP-g-PAM and then added deionized water to obtain a 2% solution (w/w). The samples were milled with potassium bromide to form very fine powder, which was then compressed into a thin pellet for analysis. Furthermore, we used the Nicolet PROTÉGÉ 460 FTIR (Thermo Scientific) to analyze the characteristic absorption profiles of the samples at a scanning range of 1–4,000 cm^{-1}. The absorption profile was the primary indicator of the substances in the sample. Moreover, we conducted thermogravimetric analysis (TGA) using a TG 209 F3 instrument (Netzsch-Gerätebau GmbH, Germany). We placed the ground samples in a nitrogen gas flow at 20 mL/min and increased the temperature from 50 to 850℃ at a rate of 10℃/min. Based on the analysis, we obtained thermal-gravimetric curves and determined the thermal stability of the compound. Finally, we observed the distribution and general morphology of ATP in the structure of the ATP-g-PAM using a SUPRA55 scanning electron microscope (SEM) (Carl Zeiss AG, Germany) and a JEM-2100 high-resolution transmission electron microscope (TEM) (JEOL, Ltd., Japan).

2.3. Microbial enrichment

We obtained liquid from the enriched nitrifying bacteria as follows: First, we collected an activated sludge sample from the biochemical reaction tank of a wastewater treatment plant. The sludge sample was then added to 2 L nitrifier enrichment culture [$(NH_4)_2SO_4$—5 g, NaCl—2 g, $FeSO_4$—0.04 g, NaH_2PO_4—1 g, $MgSO_4{\cdot}H_2O$—0.5 g, distilled water—1 L, pH 7.2, sterilized at 121℃ for 20 min]. The incubation area was aerated, and the temperature was maintained at 28–30℃. The culture was replaced every other day by settling and decanting the upper half of the supernatant. pH level remained between 7.2 and 8. After 28 d of incubation, the culture was enriched.

2.4. Batch test of ammonium removal

Several water samples were gathered from various urban rivers in Changzhou City (Jiangsu, China). These rivers ranged from lightly polluted to heavily polluted (Fig. 1). In these samples, chemical oxygen demand ranged from 60.65 to 85.47 mg/L; total nitrogen ranged between 5.47 and 16.91 mg/L; total phosphorus ranged from 0.45 to 1.25 mg/L; and ammonia-nitrogen ranged between 3.12 and 12.53 mg/L as per the measure presented by [33] (Table 1). The samples were flocculated and immobilized as follows: We added 1% nitrifying bacteria culture (2.5×10^7 cell/mL) and 1 g acid-modified ATP to a 500 mL water sample. The mixture was slowly agitated to promote adsorption. 1% (w/v) ATP/PAM hybrid flocculant was then incorporated. The flask was agitated rapidly (250–300 r/min) for 30 s and then slowly (60 r/min) for 5 min. Afterward, it was precipitated for 30 min. The fine floccules, along with the immobilized nitrifying bacteria, remained in the flask for 9 d. To measure the ammonium content, samples (1 mL) were taken every 2 d (500 mL in total). Equal amounts of microbes were obtained to compare the novel immobilization method involving ATP-g-PAM and suspended bacteria with the traditional method of immobilization [polyvinyl alcohol (PVA)–boric acid)] [34].

3. Results and discussion

3.1. Optimal synthesis condition of the ATP/PAM hybrid flocculant

The synthesis, stability, and characteristics of the ATP/PAM flocculant are significantly affected by

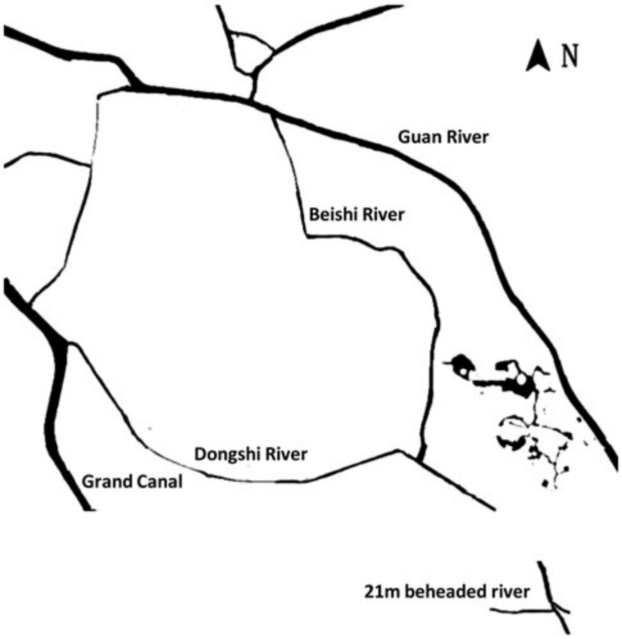

Fig. 1. Map of the sampling river.

Table 1
Contaminant concentrations in water samples

Samples	Rivers	Ammonium/mg L^{-1}	COD/mg L^{-1}	TN/mg L^{-1}	TP/mg L^{-1}
Sample 1	21 m beheaded river	16.27 ± 1.2	85.47 ± 2.5	16.91 ± 0.8	1.25 ± 0.08
Sample 2	21 m beheaded river	12.28 ± 0.8	80.25 ± 0.8	15.25 ± 0.5	0.88 ± 0.06
Sample 3	Guan River	7.04 ± 0.3	69.32 ± 3.1	10.63 ± 1.2	0.65 ± 0.03
Sample 4	Beishi River	7.40 ± 1.6	75.15 ± 2.2	8.21 ± 0.8	0.48 ± 0.05
Sample 5	Beishi River	3.67 ± 0.5	60.65 ± 2.5	5.47 ± 0.5	0.45 ± 0.09

reaction time and the amounts of AM used as monomers, initiators (mass ratio $FeSO_4$:$NaHSO_3$ = 1:5), and ATP. Thus, we optimized the synthesis condition given different reaction times and amounts of AM, initiators, and ATP.

3.1.1. *Effect of the amount of monomer mass loading*

We prepared samples of the ATP/PAM hybrid flocculant by loading AM monomer mass ranging from 10 to 20%. The other synthesis conditions were fixed (10.5×10^{-4} mol/mol AM initiator concentration, mass ratio $FeSO_4$:$NaHSO_3$ = 1:5, and 2% ATP mass loading relative to the amount of AM). As shown in Fig. 2(a), the increase in monomer mass loading initially enhanced viscosity, which reached its peak at 15% monomer loading. However, viscosity decreased afterward. As monomer mass increased, the polymerization reaction accelerated, and additional monomers were incorporated into the polymer matrices. Moreover, viscosity increased with the percentage of monomer conversion, thus reflecting live polymerization. As monomer loading increased further, the resultant increase in part of the reacting medium caused a local cage effect [35]. This cage effect prevented primary radicals, which were released by initiator molecules, from making contact with the monomers. Polymerization decelerated when initiator concentration decreased. In various parts of the reaction system, excessive polymerization heat may have reduced product viscosity, along with local differentiation [36].

3.1.2. *Effect of initiator concentration*

The ATP/PAM hybrid flocculant was produced using an initiator (mass ratio $FeSO_4$:$NaHSO_3$ = 1:5) with concentrations varying from 7×10^{-4} to 21×10^{-4} mol/mol AM. Other synthesis conditions were fixed (15% monomer mass loading, 5 h reaction time, 2% ATP mass loading relative to the amount of AM). As shown in Fig. 2(b), viscosity was high given a low initiator concentration. Moreover, the viscosity of the hybrid flocculant first increased then decreased with the increase in initiator concentration. Polymerization was initiated and sustained by free radicals [37]. When monomer amount is fixed, the availability of radicals was the dominant factor in the polymerization reaction [38]. Hence, a high initiator concentration enhanced the efficiency of monomer conversion. As a result, the reaction rate increases along with product viscosity. However, the reaction occurred too quickly; thus, the reaction heat did not dissipate. Consequently, temperature increased and the viscosity decreased significantly.

3.1.3. *Effect of reaction time*

Fig. 2(c) shows the change in product viscosity relative to varied reaction times. Reaction time ranged from 2 to 6 h when the conditions were fixed at 15% monomer mass loading, 10.5×10^{-4} mol/mol AM initiator concentration, mass ratio of $FeSO_4$:$NaHSO_3$ = 1:5, and 2% ATP. The specific viscosity of the product increased slightly with reaction time. The autoacceleration effect prolonged the lifespan of side chain radicals, thereby encouraging the generation of AM monomers in chain growth. As a result, molecular weight was enhanced. Nonetheless, radical diffusion limits heterogeneous polymerization through its slow kinetics and controls the molecular weight of the product [36].

3.1.4. *Effect of ATP mass loading amount*

Specific viscosity was also affected by the amount of ATP, as depicted in Fig. 2(d). ATPs are composed of AM monomer mass ranging from 0.5 to 3% with a monomer concentration of 15%, initiator concentration 10.5×10^{-4} mol/mol AM, mass ratio $FeSO_4$:$NaHSO_3$ = 1:5, and a reaction time of 5 h. With the increase in ATP amount, specific product viscosity first increased and then decreased. This peak viscosity corresponded to 2% ATP dosage. During grafting, the ATP particles may act as the core of the micro-crosslinking polymer

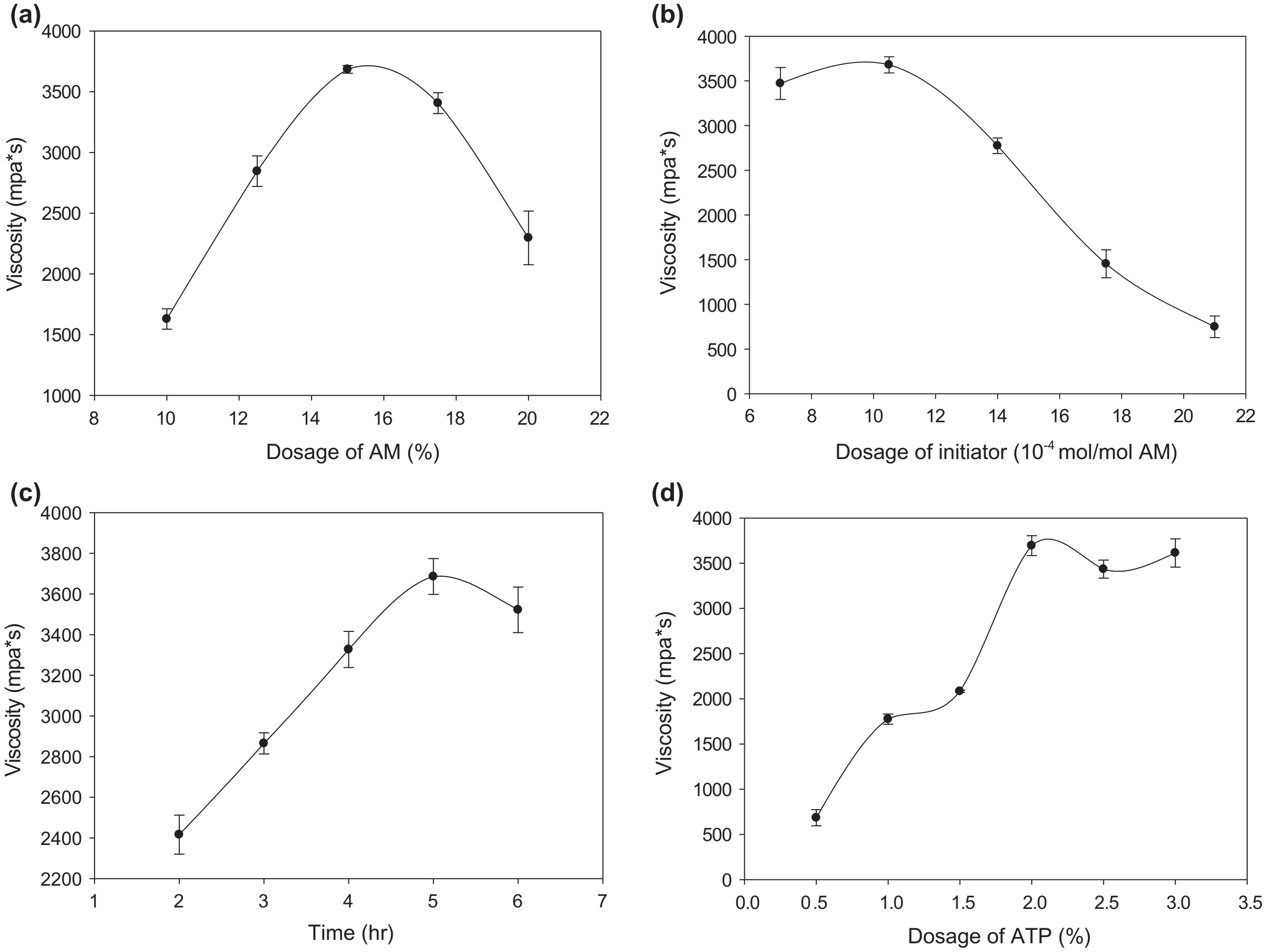

Fig. 2. Optimal synthesis condition of the ATP/PAM hybrid flocculant: (a) amount of monomer mass loading; (b) initiator concentration; (c) reaction time; and (d) ATP mass loading amount.

system [39]. This core had a high affinity for polar functional groups, such as –NH_2 and –OH and polymer chains. The polymers were enlarged as a result of polymer chain sorption on the surface, and their hydrodynamic volume increased. Thus, viscosity was enhanced. However, the intrinsic viscosity of the polymerization unit dropped given a certain dosage of ATP. As the crosslink extends and physical adsorption strengthens, the chains in the polymer matrices congregate, thereby reducing hydrodynamic volume [40].

3.2. Characterization and comparison of ATP-g-PAM

3.2.1. Structural characterization of ATP/PAM using FTIR spectra

Under the optimal condition of 15% AM monomer, 10.5×10^{-4} mol/mol AM initiator, 2% ATP, and 5 h reaction time, the ATP-g-PAM was synthesized and characterized using FTIR spectra. Fig. 3 shows the FTIR spectra before and after the formation of the ATP-g-PAM hybrid flocculant. According to the infrared PAM spectrum, the stretching and vibration absorption peaks of VN-H were observed at 3,432 cm^{-1}, the characteristic absorption peak of amide carbonyl at 1,666 cm^{-1}, the characteristic absorption peaks of methylene at 2,925 and 2,854 cm^{-1}, and the vibration absorption of δ_{CH2} at 1,455 cm^{-1}. These observations confirmed that the polymer was composed of PAM. On the spectrum of the synthesized hybrid flocculant, the asymmetric stretching vibration peaks of C–H were observed at 2,855 and 2,926 cm^{-1} and its deformation vibration at 1,455 cm^{-1}. The spike close to 1,656 cm^{-1} reflected the hydroxide groups (–OH) from the absorbed ATP water, whereas the neighboring spike close to 1,625 cm^{-1} indicated –OH generated by the

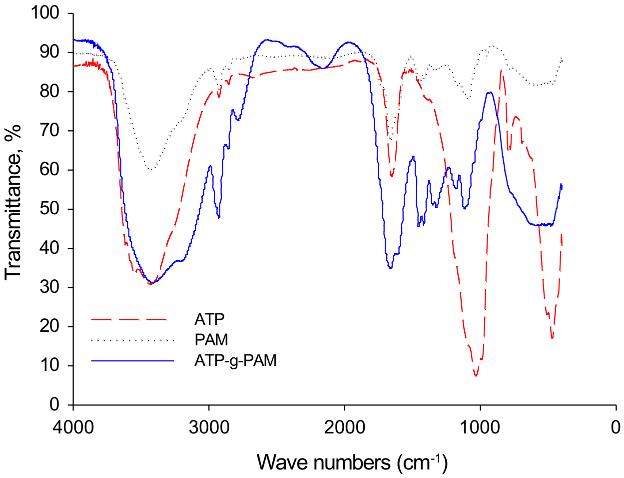

Fig. 3. FTIR spectra of PAM and ATP-g-PAM.

coordinated water. The absorption peak at 1,452 cm^{-1} was induced by Lewis acids. Furthermore, the two new absorption peaks at 1,049 and 993 cm^{-1} were attributed to the asymmetric and symmetric stretching vibrations of Si-O, respectively, and denoted the grafting and polymerization of the AM monomers.

3.2.2. TGA of ATP/PAM

The slight weight loss at 200˚C was attributed to the escape of free water. Moreover, both PAM (Fig. 4(a)) and the hybrid flocculant (Fig. 4(b)) were moderately stable thermally. For both materials, weight loss was most prominent above 300˚C, at which the PAM and ATP-g-PAM peaks decreased at 382.5 and 386.9˚C, respectively. This reduction was correlated with the different temperatures required for the initial decomposition of the materials. At above 600˚C, the residual weight percentage of PAM (18.22%) was lower than that of the hybrid flocculant (31.99%). The improved stability was a result of ATP incorporation during polymerization. In the polymer matrix, these inorganic clay particles formed a heat barrier and significantly decelerated internal heat conductance and thermal decomposition. This "barrier effect" was key to improving the heat stability of the hybrid flocculant.

3.2.3. Electron microscope scan of ATP/PAM

The TEM image of the ATP-g-PAM hybrid flocculant (Fig. 5(a)) shows that the surface of the hybrid flocculant was flat. The dark areas on the image (Fig. 5(b)) represent the crystalline bars and bundles of ATP, which contain the distributed nano-acicular fibers in the PAM matrix. This image confirms that the hybrid flocculant was well synthesized.

3.2.4. Initial synthesizing mechanism of ATP/PAM

Numerous studies have mainly considered clay modification in the generation of synthetic polymer from clay and AM monomers [41–43]. Functional groups are grafted to clay particles through ionic exchange. These functional groups are activity centers of polymerization reactions once they are activated by initiators. During polymerization, AM monomers intercalate *in situ* at these centers to form ionic-bonded structures. However, other researchers have developed methods that do not require clay modification. They report that abundant and hydrophilic silicon hydroxyl groups on the clay surface can facilitate the grafting of alkene monomers. After initiator activation, the clay releases free radicals that precipitate the polymerization of AM monomers [24,44]. At the structural hydroxyl groups, Bronst acid sites can form in the layered ATP crystal structure. Mg^{2+} and Al^{3+} ions can exchange easily with exogenous metal ions, and the exposed Al^{3+} ions are potential sites of Lewis acid. Most Lewis acids are produced through the Al^{3+} ions on the edge of crystal layers; some of these acids are uncoordinated, whereas the others exposed by dehydration. Moreover, the possible sources of Bronst acids are as follows: (1) weakly acidic Si–OH and Al–OH that are exposed at the edges of crystal layers or end-face imperfections; (2) negatively charged centers in the layers (particularly the localities of Si–O–Al, where tetrahedral Si atoms are replaced by Al atoms) that contain counteracting H^+ but have not been bound to columns/layers; (3) polarized water molecules on the mineral surface; and (4) H^+ from the acid modification of ATP. Following this modification, the surface acid centers serve as a potential functional core to catalyze multiphase catalytic reactions [45–47]. In this study, therefore, modified ATP not only provides the required substrate for AM grafting, but also the activation zones for polymerization the given the acid sites of Bronst and Lewis. Furthermore, the released Al^{3+}, Mg^{2+}, and possible Fe^{2+} from reductants may form complexes with peptide amine groups. These complexes can integrate further with the chain growth radicals from PAM by altering the activity of the radicals and initiating the polymerization reaction. This process improves reaction rate and product viscosity as well [48]. In conclusion, the addition of ATP facilitates AM polymerization.

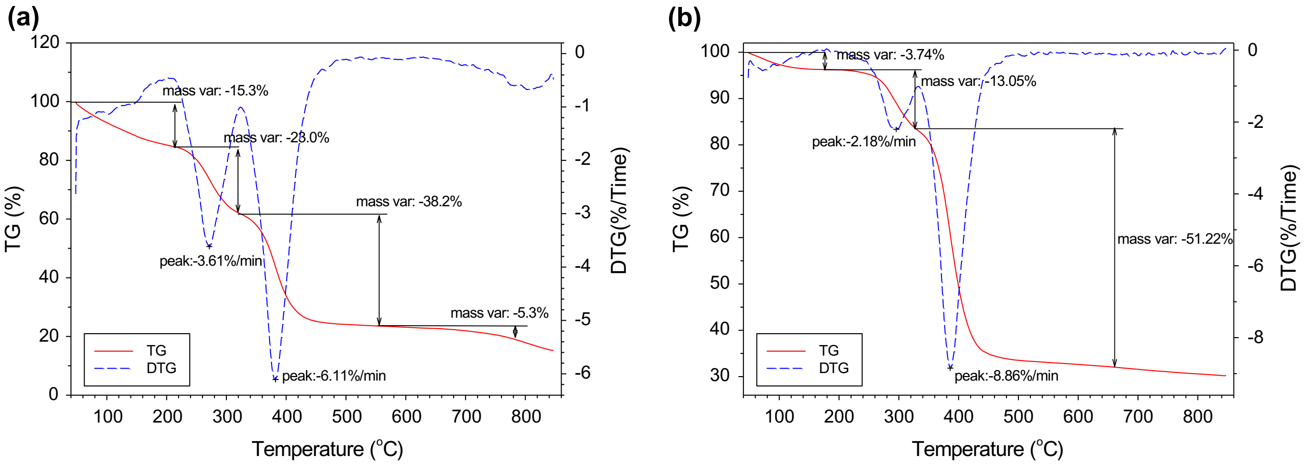

Fig. 4. TGA of (a) PAM and (b) ATP-g-PAM.

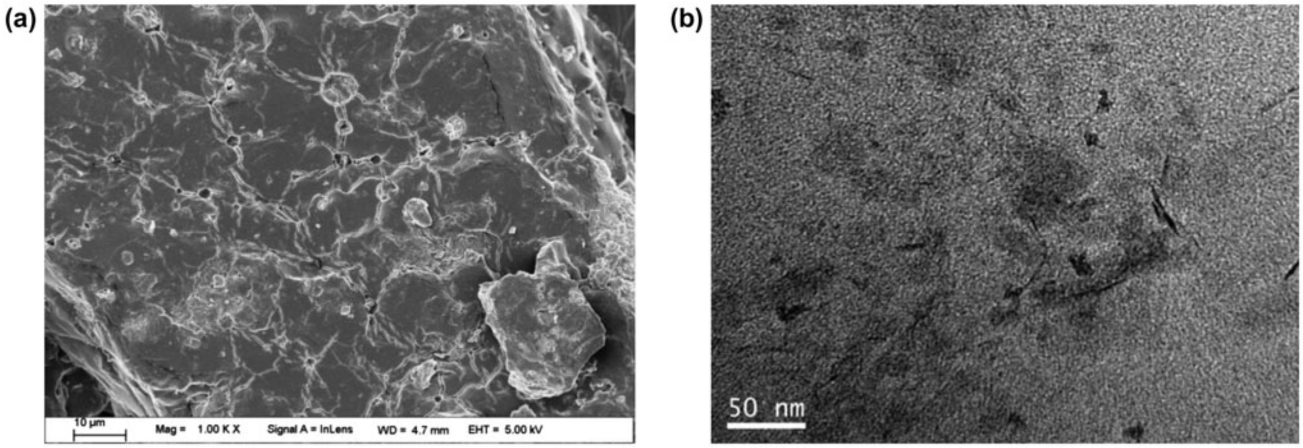

Fig. 5. Electron microscope scan of ATP/PAM: (a) SEM and (b) TEM.

3.3. Removal of ammonia from surface water

To investigate the use of ATP/PAM in the flocculation and immobilization of nitrifying microbes for ammonium removal, surface water samples were obtained from urban rivers that ranged from lightly contaminated to heavily contaminated. Fig. 6 displays the decreasing ammonia concentration during flocculation and immobilization. During the first 35 min of flocculation and precipitation, the ammonium removal rate ranged from 14.9 to 33.9%, potentially as a result of both flocculation and adsorption. The adsorption capacity of ATP was 0.69 mg/g in this study. As per TGA (Fig. 4) and scanning (Fig. 5), the structure of ATP-g-PAM synthesized stably. This stable synthesis facilitates the effective and rapid removal of ammonium through flocculation and adsorption. In addition, the micro-ducts of ATP formed into honeycomb-shaped cross-sections that basically combined countless parallel tubular ducts with equal cross-sections. This unique structure, which is similar to a molecular sieve, enhances the adsorption capacity of ATP.

Fig. 6 also depicts the batch test performance of the hybrid flocculant with immobilized microbes. In the first 2 d, we observed minor changes. Following this period, ammonia removal was accelerated, and the percentage of removal ranged from 69.4 to 82.6%. As per the scanning result (Fig. 5), the ATP-g-PAM carrier generated numerous sorption sites. Moreover, its large specific surface area accommodated the attachment of even ammonia and substrates, thereby enhancing the metabolic environment of the microorganisms. As observed in this study, the nitrifying bacteria in the ATP-g-PAM carrier reached 10^8 cell/mL, playing an important role in ammonia removal through nitrification process. Furthermore, ATP increased flocculant permeability,

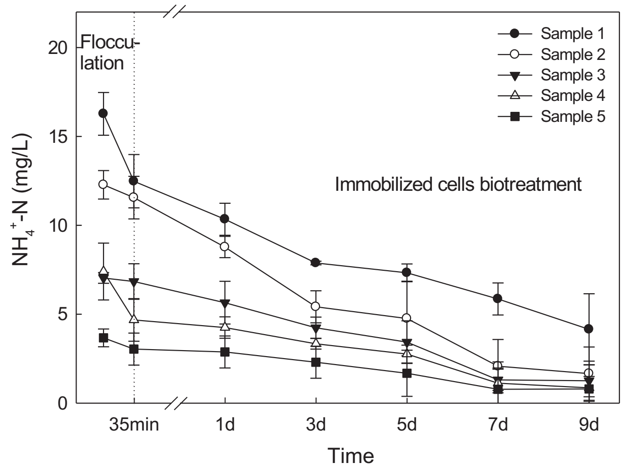

Fig. 6. Ammonium biotreatment involving flocculation with immobilized microbes.

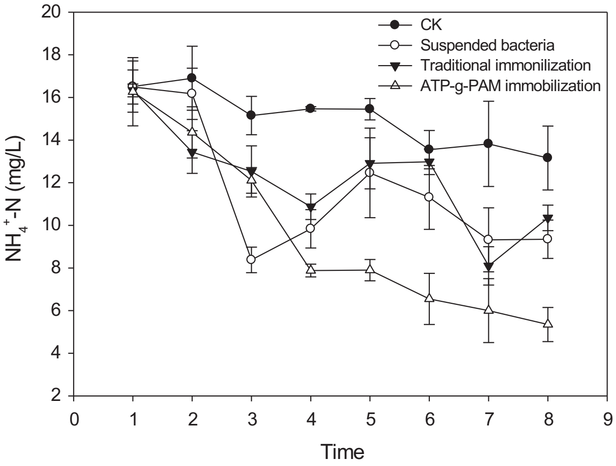

Fig. 7. Comparison of the ATP-g-PAM immobilization method with methods of suspended bacteria and traditional immobilization (PVA–boric acid).
Note: CK denotes the control sample without additional bacteria.

which improved the mass transfer of oxygen and other substrates from the surface to the core. This improvement was conducive to bacterial growth and nitrogen removal. After the 2 d adaptive period, the efficiency of ammonia removal efficiency increased. We also compared this novel immobilization method involving ATP-g-PAM and suspended bacteria with the traditional method of immobilization (PVA–boric acid) (Fig. 7). Ammonium also decreased slightly in the control sample (CK). Although the amount of suspended bacteria initially decreased significantly and more quickly in the proposed method than in the others, ammonium concentration increased again at a later period. This finding may be attributed to the instability and death of the suspended bacteria. Therefore, the proposed method removed ammonium more effectively than the traditional immobilization method because of its high specific surface area and the dense pores of the immobilized pellets it generates. These pellets act as sustainable carriers for bacteria with high metabolic activities.

The immobilization process that integrates adsorption and flocculation [49–51] is technologically advantageous. In our study, the modified ATP is the main body for the initial adsorption of ammonia and other organic pollutants. This non-toxic material does not induce secondary pollution. Furthermore, the specific surface area of ATP was expanded through acid modification to produce additional sorption sites that facilitated microbial growth and reproduction. Through the "bridging" mechanism [52], active functional groups caused the adsorption of the laboratory-constructed hybrid flocculant onto the suspended ATP micro-particles. This process also integrated the ATP particles with other organic matters to form enlarged particles. Under flocculation and precipitation, both free and adsorbed active microorganisms settled in the three-dimensional matrices. Given its stable bacteriological growth conditions, efficient ammonia removal, and enhanced mechanical strength, this immobilization method effectively removes ammonium from surface water. For environment safety, however, the microbial flocculant may be incorporated further with nitrifying bacteria during flocculation with immobilized cells for nitrogen removal.

Acknowledgments

This work was supported by National Natural Scientific Foundation of China (No. 41101233, No. 41371256), Jiangsu Province Natural Scientific Foundation (BK2011233), Major Science and Technology Program for Water Pollution Control and Treatment (2012ZX07301001), and Qing Lan Project of Jiangsu (No. JSQL2012).

References

[1] J. Wu, S. Cheng, Z. Li, W. Guo, F. Zhong, D. Yin, Case study on rehabilitation of a polluted urban water body in Yangtze River Basin, Environ. Sci. Pollut. Res. 20 (2013) 7038–7045.

[2] Y. Xie, Z. Xiong, G. Xing, G. Sun, Z. Zhu, Assessment of nitrogen pollutant sources in surface waters of Taihu Lake Region, Pedosphere 17 (2007) 200–208.

[3] Y. Wu, Y. Wu, Removal of ammonia nitrogen by combining the ammonia stripping with electrochemical oxidation, Adv. Mater. Res. 664 (2013) 454–457.
[4] H. Huang, Q. Song, W. Wang, S. Wu, J. Dai, Treatment of anaerobic digester effluents of nylon wastewater through chemical precipitation and a sequencing batch reactor process, J. Environ. Manage. 101 (2012) 68–74.
[5] Z. Du, P. Ren, Ammonia nitrogen removal from chlor-alkali chemical industry wastewater by magnesium ammonium phosphate precipitation method, Adv. Mater. Res. 573–574 (2012) 1096–1100.
[6] J.H. Koon, W.J. Kaufman, Ammonia removal from municipal wastewaters by ion exchange, J. Water Pollut. Control Fed. 47 (1975) 448–465.
[7] T. Parvanova-Mancheva, V. Beschkov, Microbial denitrification by immobilized bacteria *Pseudomonas denitrificans* stimulated by constant electric field, Biochem. Eng. J. 44 (2009) 208–213.
[8] X. Wang, J. Wang, Removal of nitrate from groundwater by heterotrophic denitrification using the solid carbon source, Sci. China Ser. B: Chem. 52 (2009) 236–240.
[9] C.D. Scott, Immobilized cells: A review of recent literature, Enzyme Microb. Technol. 9 (1987) 66–72.
[10] A. Magrí, M.B. Vanotti, A.A. Szögi, Anammox sludge immobilized in polyvinyl alcohol (PVA) cryogel carriers, Bioresour. Technol. 114 (2012) 231–240.
[11] K. Isaka, Y. Kimura, T. Osaka, S. Tsuneda, High-rate denitrification using polyethylene glycol gel carriers entrapping heterotrophic denitrifying bacteria, Water Res. 46 (2012) 4941–4948.
[12] A. Cheikh, A. Yala, N. Drouiche, N. Abdi, H. Lounici, N. Mameri, Denitrification of water in packed beds using bacterial biomass immobilized on waste plastics as supports, Ecol. Eng. 53 (2013) 329–334.
[13] S.A. Covarrubias, L.E. De-Bashan, M. Moreno, Y. Bashan, Alginate beads provide a beneficial physical barrier against native microorganisms in wastewater treated with immobilized bacteria and microalgae, Appl. Microbiol. Biotechnol. 93 (2012) 2669–2680.
[14] X. Bai, Z. Ye, Y. Li, L. Zhou, L. Yang, Preparation of crosslinked macroporous PVA foam carrier for immobilization of microorganisms, Process Biochem. 45 (2010) 60–66.
[15] K. Isaka, Y. Kimura, T. Yamamoto, T. Osaka, S. Tsuneda, Complete autotrophic denitrification in a single reactor using nitritation and anammox gel carriers, Bioresour. Technol. 147 (2013) 96–101.
[16] S.A. Ansari, Q. Husain, Potential applications of enzymes immobilized on/in nano materials: A review, Biotechnol. Adv. 30 (2012) 512–523.
[17] L.E. De-Bashan, Y. Bashan, Immobilized microalgae for removing pollutants: Review of practical aspects, Bioresour. Technol. 101 (2010) 1611–1627.
[18] W. Zheng, L.C. Zhou, Y.Y. Xu, Z.F. Ye, Y.F. Li, Progress on design, preparation of high performance carriers and their application of immobilized microorganism for wastewater treatment. Functional materials and applications, in: Proceedings of the 7th National Conference on Functional Materials and Applications, Changsha, China, October 18, 2010.
[19] Z. Yang, X. Liu, B. Gao, S. Zhao, Y. Wang, Q. Yue, Q. Li, Flocculation kinetics and floc characteristics of dye wastewater by polyferric chloride–poly-epichlorohydrin–dimethylamine composite flocculant, Sep. Purif. Technol. 118 (2013) 583–590.
[20] Y. Sun, H. Zheng, M. Tan, Y. Wang, X. Tang, L. Feng, X. Xiang, Synthesis and characterization of composite flocculant PAFS–CPAM for the treatment of textile dye wastewater, J. Appl. Polym. Sci. 131 (2014), doi:10.1002/APP.40062.
[21] Y. Wang, F. Zhang, Y. Chu, B. Gao, Q. Yue, The dye or humic acid water treatment and membrane fouling by polyaluminum chloride composited with sodium alginate in coagulation–ultrafiltration process, Water Sci. Technol. 67 (2013) 2202–2209.
[22] N. Li, R. Bai, C. Liu, Enhanced and selective adsorption of mercury ions on chitosan beads grafted with polyacrylamide via surface-initiated atom transfer radical polymerization, Langmuir 21 (2005) 11780–11787.
[23] I.G. Shibi, T.S. Anirudhan, Synthesis, characterization, and application as a mercury(II) sorbent of banana stalk (*Musa paradisiaca*)-polyacrylamide grafted copolymer bearing carboxyl groups, Ind. Eng. Chem. Res. 41 (2002) 5341–5352.
[24] Q. Chang, X. Hao, L. Duan, Synthesis of crosslinked starch-graft-polyacrylamide-co-sodium xanthate and its performances in wastewater treatment, J. Hazard. Mater. 159 (2008) 548–553.
[25] W.L. Haden, I.A. Schwint, Attapulgite: Its properties and applications, Ind. Eng. Chem. 59 (1967) 58–69.
[26] W.X. Shi, Y.S. Duan, X.S. Yi, S. Wang, N. Sun, C. Ma, Biological removal of nitrogen by a membrane bioreactor attapulgite clay system in treating polluted water, Desalination 317 (2013) 41–47.
[27] X.S. Yi, Z.W. Zhao, W.X. Shi, Y.S. Duan, N. Sun, C. Ma, Y.Z. Xie, Organic pollutants variation and antifouling enhancement with attapulgite clay addition in MBR treating micro-polluted surface water, Chem. Eng. J. 223 (2013) 891–898.
[28] H. Cui, Y. Qian, Q. Li, Z. Wei, J. Zhai, Fast removal of Hg(II) ions from aqueous solution by amine-modified attapulgite, Appl. Clay Sci. 72 (2013) 84–90.
[29] Y. Kong, J. Yuan, Z. Wang, S. Yao, Z. Chen, Application of expanded graphite/attapulgite composite materials as electrode for treatment of textile wastewater, Appl. Clay Sci. 46 (2009) 358–362.
[30] P. Liu, J. Guo, Polyacrylamide grafted attapulgite (PAM-ATP) via surface-initiated atom transfer radical polymerization (SI-ATRP) for removal of Hg(II) ion and dyes, Colloids Surf., A 282–283 (2006) 498–503.
[31] L. Wang, J. Sheng, Preparation and properties of polypropylene/org-attapulgite nanocomposites, Polymer 46 (2005) 6243–6249.
[32] Y. Wang, W. Wang, X. Shi, A. Wang, Enhanced swelling and responsive properties of an alginate-based superabsorbent hydrogel by sodium p-styrenesulfonate and attapulgite nanorods, Polym. Bull. 70 (2013) 1181–1193.
[33] F. Wei, Water and Wastewater Monitoring Analysis Method, fourth ed., China Environmental Science Press, Beijing, 2002.
[34] C. Jeon, J.Y. Park, Y. Yoo, Novel immobilization of alginic acid for heavy metal removal, Biochem. Eng. J. 11 (2002) 159–166.
[35] Z. Wu, W. Li, P.A. Webley, General and controllable synthesis of novel mesoporous magnetic iron oxide@carbon encapsulates for efficient arsenic removal, Adv. Mater. 24 (2012) 485–491.

[36] H. Wang, J. Cui, W. Jiang, Synthesis, characterization and flocculation activity of novel $Fe(OH)_3$–polyacrylamide hybrid polymer, Mater. Chem. Phys. 130 (2011) 993–999.

[37] R.L. Barbey, L. Lavanant, D.P.N.S. Paripovic, N. Schüwer, C. Sugnaux, S. Tugulu, Polymer brushes via surface-initiated controlled radical polymerization: Synthesis, characterization, properties, and applications, Chem. Rev. 109 (2009) 5437–5527.

[38] S. Mishra, A. Mukul, G. Sen, U. Jha, Microwave assisted synthesis of polyacrylamide grafted starch (St-g-PAM) and its applicability as flocculant for water treatment, Int. J. Biol. Macromol. 48 (2011) 106–111.

[39] H. Hou, L. Tian, Synthesis and application of organic-inorganic composite flexible architectural coatings emulsion, Appl. Mech. Mater. 357–360 (2013) 1241–1248.

[40] M.A. Malana, J. Bukhari, R. Zohra, Synthesis, swelling behavior, and network parameters of novel chemically crosslinked poly(acrylamide-co-methacrylate-co-acrylic acid) hydrogels, Des. Monomers Polym. 17 (2014) 266–274.

[41] Y. Zhao, Y. Chen, M. Li, S. Zhou, A. Xue, W. Xing, Adsorption of Hg^{2+} from aqueous solution onto polyacrylamide/attapulgite, J. Hazard. Mater. 171 (2009) 640–646.

[42] Y. Mansoori, S.V. Atghia, M.R. Zamanloo, G. Imanzadeh, M. Sirousazar, Polymer–clay nanocomposites: Free-radical grafting of polyacrylamide onto organophilic montmorillonite, Eur. Polym. J. 46 (2010) 1844–1853.

[43] S.R. Shirsath, A.P. Hage, M. Zhou, S.H. Sonawane, M. Ashokkumar, Ultrasound assisted preparation of nanoclay Bentonite–FeCo nanocomposite hybrid hydrogel: A potential responsive sorbent for removal of organic pollutant from water, Desalination 281 (2011) 429–437.

[44] P. Li, J. Zhang, A. Wang, A novel N-succinylchitosan-graft-polyacrylamide/attapulgite composite hydrogel prepared through inverse suspension polymerization, Macromol. Mater. Eng. 292 (2007) 962–969.

[45] B. Joy, S. Ghosh, P. Padmaja, M. Lalithambika, A facile 1,2 proton migration of chalcone epoxide using acid activated palygorskites, Catal. Commun. 6 (2005) 573–577.

[46] P. Pushpaletha, M. Lalithambika, Modified attapulgite: An efficient solid acid catalyst for acetylation of alcohols using acetic acid, Appl. Clay Sci. 51 (2011) 424–430.

[47] X. Zhao, Y. Meng, X. Lu, X. Li, Sol–gel synthesis and catalytic property of $Ce_{1-x}Ti_xO_2$ nanocomposites supported on attapulgite clay, J. Sol-Gel Sci. Technol. 66 (2013) 22–30.

[48] W. Baade, D. Hunkeler, A.E. Hamielec, Copolymerization of acrylamide with cationic monomers in solution and inverse-microsuspension, J. Appl. Polym. Sci. 38 (1989) 185–201.

[49] G. Rehn, C. Grey, C. Branneby, P. Adlercreutz, Chitosan flocculation: An effective method for immobilization of *E. coli* for biocatalytic processes, J. Biotechnol. 165 (2013) 138–144.

[50] Y. Li, W. Li, H. Gao, J. Xing, H. Liu, Integration of flocculation and adsorptive immobilization of *Pseudomonas delafieldii* R-8 for diesel oil biodesulfurization, J. Chem. Technol. Biotechnol. 86 (2011) 246–250.

[51] P. Lertsutthiwong, D. Boonpuak, W. Pungrasmi, S. Powtongsook, Immobilization of nitrite oxidizing bacteria using biopolymeric chitosan media, J. Environ. Sci. 25 (2013) 262–267.

[52] Y.A. Attia, Flocculation in biotechnology and separation systems, in: Proceedings of the International Symposium on Flocculation in Biotechnology and Separation Systems, San Francisco, CA, July 28–August 1, 1986.